Custom Spectral Shaping for EMI Reduction in Electronic Ballasts

Sandra Johnson, Yan Yin, Regan Zane
Colorado Power Electronics Center
University of Colorado at Boulder
Boulder, Colorado 80309-0425
sandra.johnson@colorado.edu

***Abstract*—This paper presents the use of frequency modulation (FM) as a spread spectrum technique to reduce EMI caused by high frequency electronic ballasts. Amplitude modulation (AM) effects due to ballast dynamics are counteracted by the use of uniquely shaped modulating waveforms, resulting in the elimination of power spectral density (PSD) distortion and reduced peak currents and component stress. A 12-15dB signal reduction is achieved to comply with typical FCC chimney requirements.**

Keywords-component; Ballast, EMI, Reduction, Waveshape, Flourescent.

I. INTRODUCTION

High frequency sources are used to drive discharge lamps in order to improve lumen maintenance, eliminate flicker, control lamp power and light color, increase lifetime and realize smaller and lighter ballasts. With such a source, EMI becomes a major concern. Specialized coatings and enclosures are used to reduce noise and comply with FCC regulations. Such precautions are expensive and add to the size and weight of the lamp.

Alternatively, spread spectrum techniques, such as frequency modulation (FM) and random switching, have been used extensively to reduce EMI in power supplies [1-10]. The power spectral density (PSD) is spread over a wider frequency range, thereby reducing the peak value to allow compliance with FCC regulations. Noise modulation is also used for electronic ballasts in [11] to avoid excitation of instabilities due to acoustic resonance. In [1-10], the primary concern is in attenuation of higher-order harmonics of the switching frequency to reduce cross-talk and meet FCC requirements. In the lighting electronics field, new lamp technologies including electrode-less fluorescent lamp (EFL) and ceramic metal halide (CMH) lamps operate at frequencies in the MHz range. Here the concern is the attenuation of the fundamental of the switching frequency, where the FCC has designated special output power requirements in the form of a chimney between 2.5MHz and 3MHz.

In this paper, we present the use of frequency modulation, utilizing unique modulating waveforms, for custom spectral shaping of the fundamental harmonic of electronic ballasts operating in designated FCC chimneys. Section II discusses the theory of FM, parameters relevant to EMI signal reduction, and reviews typical modulating waveforms and their resulting PSDs. Experimental results for a compact fluorescent lamp (CFL) are presented in Section III. Details of the effects of amplitude modulation (AM) due to the ballast dynamics, causing PSD distortion, are discussed, and unique multi-slope modulating waveforms utilized to correct AM effects are shown. The EMI reduction technique presented here uses a new experimental test platform based on the Xilinx FPGA, offering direct digital frequency control for hardware realization of the control waveforms.

This work is sponsored by General Electric Co. Global research, through the Colorado Power Electronics Center and is cofunded by the Department of Energy's National Energy Technology Laboratory under Cooperative Agreement DE-FC26-02NT41252

I. FREQUENCY MODULATION (FM) WAVESHAPING

Frequency modulation has been traditionally used to manipulate a high frequency carrier waveform to send information wirelessly. This technique results in the spreading of 98% of the carrier signal's power over a user specified bandwidth. Its simplicity and ability to control signal energy in this way, makes FM a good candidate to reduce noise due to high frequency sources.

A. FM Theory

In frequency modulation, the frequency of a carrier signal is changed to convey information. Equation (1) shows the resulting signal when a sinewave is used to vary the carrier frequency.

$$y(t) = A_c \cos(2\pi f_c t + \frac{k_f A_m}{f_m} \sin 2\pi f_m t) \qquad (1)$$

The carrier signal is a cosine waveform with an amplitude of A_c, and a frequency of f_c. Its instantaneous frequency is affected by the modulating waveform's frequency, f_m, and amplitude, A_m, and a proportionality constant k_f. The maximum frequency deviation, ΔF, sets the bandwidth over which the signal energy is spread. The peak-to-peak swing of the modulating waveform amplitude determines the total bandwidth or ΔF. The modulating index, β, is the ratio of ΔF and f_m and is given in (2)

$$\beta = \frac{k_f A_m}{f_m} = \frac{\Delta F}{f_m} \qquad (2)$$

The spectral content of a frequency modulated signal, having a sinewave as its modulating waveform, is best described using Bessel functions [12]. The resulting signal consists of a spectral component at the carrier frequency and an infinite number of sidebands whose amplitudes are proportional to $J_n(\beta)$ (the Bessel function of the first kind and nth order), spaced f_m apart. For a sufficiently large n, $J_n(\beta)$ is negligible, resulting in a finite number of significant sidebands. More specifically, $J_n(\beta)$ is negligible for $n > \beta+2$, and therefore the number of significant sidebands is $\beta+2$. The bandwidth of an FM signal is given in (3). In the case of wideband FM (WBFM), $\Delta F >> f_m$ and the bandwidth can be approximated as $2\Delta F$.

$$BW = 2nf_m = 2(\beta + 2)f_m = 2(\Delta F + 2f_m) \approx 2\Delta F \quad (3)$$

As β increases, the number of sidebands increases, resulting in signal energy that is more evenly distributed in the bandwidth. An even distribution of signal energy provides a greater overall reduction of the fundamental carrier frequency amplitude. As illustrated in Figure 1, β is increased by increasing ΔF, or decreasing f_m.

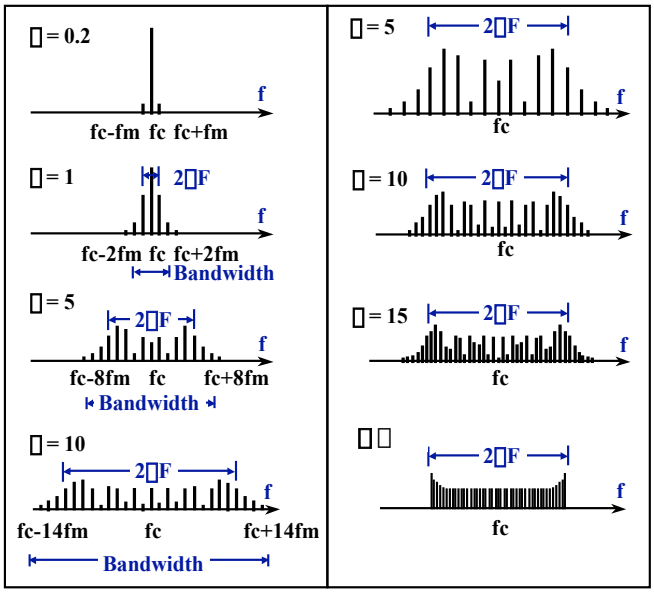

Figure 1. The effects of changing β on the spectral content of the modulated signal with (a) fixed f_m and varied ΔF and (b) fixed ΔF and varied f_m

A. Waveshaping

The PSD of a frequency modulated signal, utilizing a sinewave as the modulating waveform, is well defined mathematically. From an intuitive standpoint, the PSD can be characterized as an amount of energy at a frequency determined by the length of time spent (or dwelled) at that frequency. Figure 2(a) shows a sinewave as the modulating waveform and the resulting frequency modulated PSD of the carrier signal. The dwell-time at each frequency is directly related to the slope of the sinusoid. The slope becomes steeper at the zero crossing which maps to the carrier center frequency. At the carrier frequency, energy of the PSD is at a minimum. At the edges of the spreading bandwidth ($f_c+\Delta F$ and $f_c-\Delta F$), the slope of the sinusoid is the shallowest equating to a longer dwell-time. It is at these bandwidth edges where more energy appears in the PSD, resulting in peaks that may make it difficult to comply with a typical FCC chimney shown in Figure 2 by dotted lines. Figure 2(b) shows the resulting PSD of the frequency modulated carrier when the modulating waveform is a squarewave. The signal dwells mainly at the minimum and maximum frequency values of ΔF. This leads to a PSD having most of its energy occupying the bandwidth edges, and does not provide a good solution for FCC compliance. Figure 2(c) shows the same frequency modulated carrier utilizing a ramp (or sawtooth) as its modulating waveform. The ramp has a constant slope over its entire period, allowing for an equal dwell-time over all frequencies in the bandwidth. The resulting PSD's spectral content has energy equally distributed across the band, resulting in a good candidate for FCC compliance. All PSD waveforms in Figure 2 are simulated in Matlab, utilizing the Welch method for translation into the frequency domain.

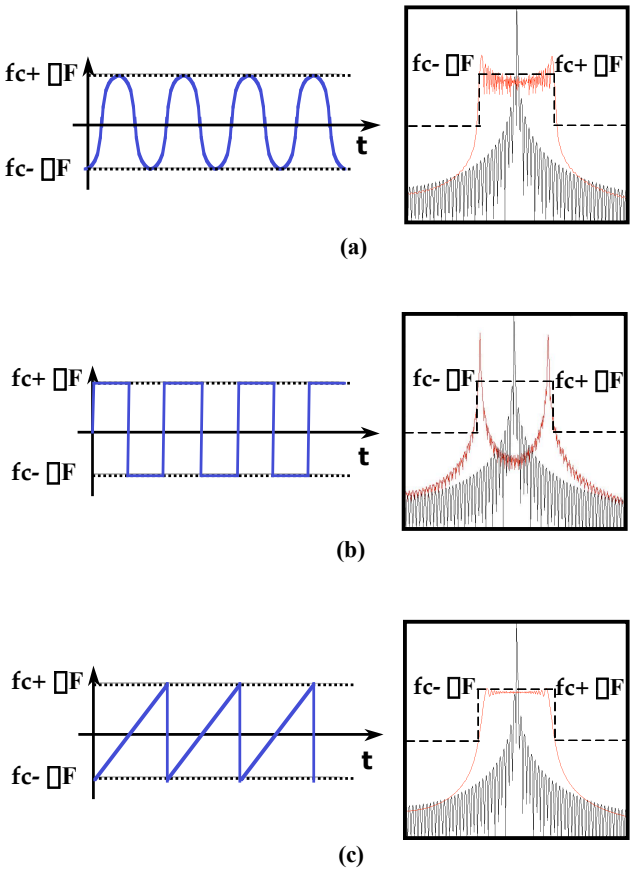

Figure 2. Resulting PSD of a frequency modulated carrier having a modulating signal of the form of (a) a sinewave, (b) a squarewave and (c) a ramp or sawtooth wave.

I. EXPERIMENTAL RESULTS

A. *Test Platform for Direct Digital Frequency Control*

In order to provide direct digital control of the electronic ballast, a test platform was developed based on the Insight/Memec development board for the Xilinx Virtex II FPGA [13]. This test platform provides rapid prototyping of custom digital modulation techniques with realistic hardware implementation, demonstrating commercial feasibility of the proposed concept. An 8-bit digitally controlled oscillator (DCO) was implemented in the FPGA using standard digital Verilog coding and fully automated synthesis and place-and-route. The DCO is based on an internal timer and state machine with time resolution of 10ns. This new platform enables significant freedom for investigation of frequency modulation techniques.

The FPGA board varies the switching frequency of the high frequency source over a predetermined spreading bandwidth range (f_s+ □F to $f_{sß}$- □F). The spreading frequencies are stepped through using a counter with a minimum resolution of 10 nsec per clock period or count, where the period of the desired frequency is given in (4).

$$T_{freq} = (\#\,counts)(10n\,\mathrm{sec}/count) \qquad (4)$$

Figure 3 shows a resulting FPGA generated ramp modulating waveform. The simple approach using fixed steps in period results in non-linear steps in frequency as shown in Figure 4. A more general technique is to use a lookup table and pre-compute the desired non-linear period steps.

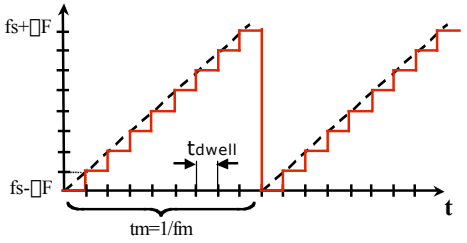

Figure 3. Resulting FPGA generated modulating waveform

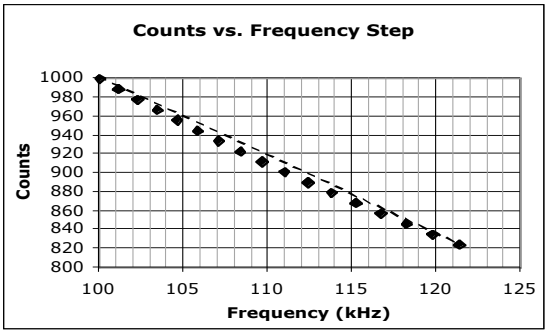

Figure 4. Resulting non-linear frequency steps utilizing counts based on 10nsec multiples

A. *Frequency Modulation of the Compact Flourescent Lamp (CFL) Source*

An experimental circuit based on a half-bridge LCC resonant inverter driving a CFL load, as shown in Figure 5, was built and tested. The setup allows for a function generator or the FPGA platform to provide the high frequency source. Both are capable of applying FM to the switching frequency. In either case, the FPGA provides the driver function with non-overlapping clocks, and a toggle switch on the board allows the user to select between the two.

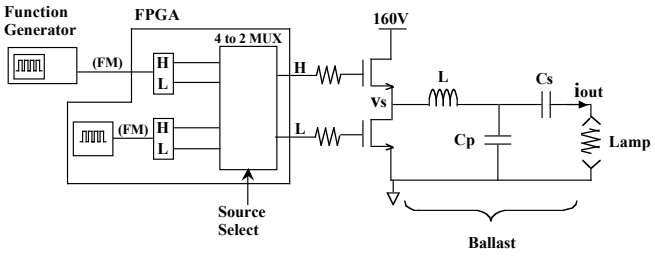

Figure 5. Experimental circuit configuration

From observing the low side gate voltage, it is evident that the FPGA successfully modulated the switching frequency as expected in Figure 6. The resulting PSD of the ballast current is shown in Figure 7. The amount of signal reduction is measured as the difference between the maximum power of the unmodulated and modulated signal PSDs at the center or switching frequency. Signal reduction increases as □ increases, and the reduction trend can be seen in Figure 8.

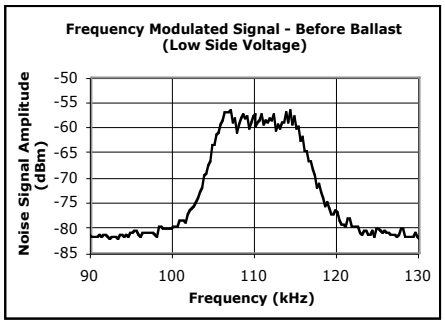

Figure 6. Resulting frequency modulated source (low side voltage)

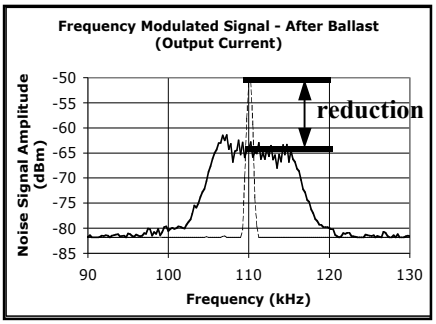

Figure 7. Frequency modulated ballast current

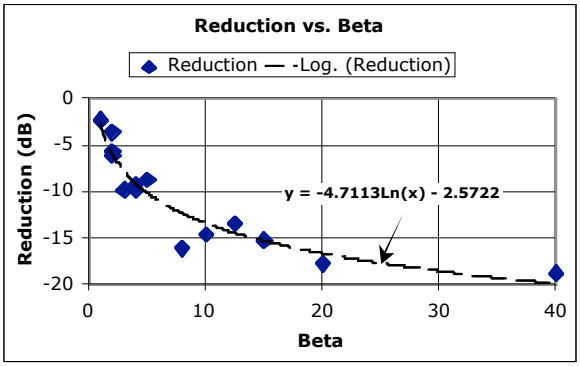

Figure 8. Reduction trend with increasing □, based on measured values

The modulated ballast current PSD shows a distortion characterized by a slight tilt of the signal when compared to the PSD of the modulated low side gate voltage. This distortion is due to the dynamics of the ballast, which acts as a filter, causing amplitude modulation as a secondary effect. In fact, the output power of electronic ballasts are commonly regulated through frequency control due to the AM effect.

A typical steady-state characteristic (based on sinusoidal approximation [14]) of the electronic ballast is given in (5) and shown in Figure 9. The x-axis is the steady-state switching frequency and the y-axis is the gain for the input voltage (midpoint voltage) to the output current. Small perturbations around the nominal switching frequency result in AM.

$$G(j\omega) = \frac{i_{out}(j\omega)}{v_s(j\omega)} = \frac{jwC_s}{1 + jwC_sR + (j\omega)^2 L(C_s + C_p) + (j\omega)^3 LC_sC_pR} \quad (5)$$

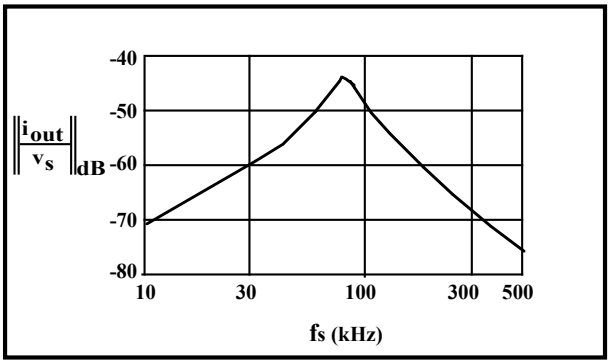

Figure 9. Ballast characteristic: gain of input voltage to output current vs. switching frequency

The amount of amplitude modulation increases with increasing spreading bandwidth (2□F). The modulation index or depth of AM is given in (6), and can be measured from the time domain representation of the ballast current as shown in Figure 10.

$$\%AM = \frac{I_{max} - I_{min}}{I_{max} + I_{min}} x100\% \quad (6)$$

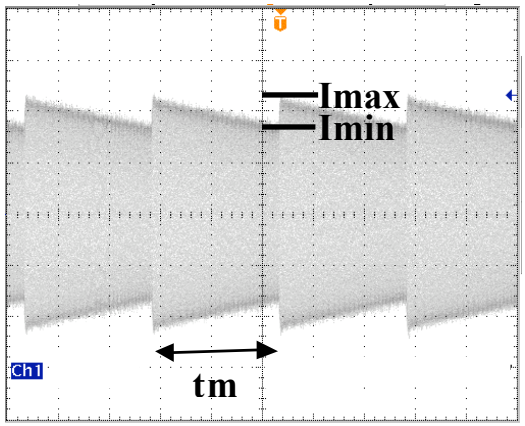

Figure 10. Amplitude modulation of the ballast current

The current crest factor (CCR) is the ratio of the peak current to the RMS current and ideally is equal to one. Increasing the depth of AM causes increasing peak current leading to significant component stress, reducing lamp life and distorting the resultant PSD. Large variations in voltage and current, due to a large depth AM, causes audible vibration and flicker.

A trade-off arises between depth of AM and the amount of signal reduction. The maximum frequency deviation (□F) is set for a predetermined spreading bandwidth. The FM modulation index, □, must be increased to obtain the desired signal reduction and at the same time decreased to reduce depth of AM. Figure 11 shows the effects of varying f_m with fixed □F. A small value for f_m yields a high □ along with a large signal reduction and large depth of AM. As f_m increases, □ decreases leading to a decreased depth of AM at the cost of signal reduction.

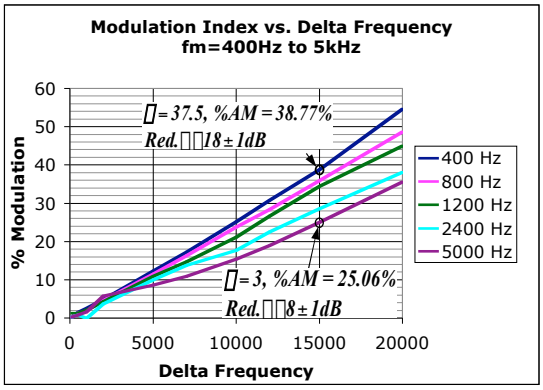

Figure 11. Change in depth of AM with fixed □F and varying f_m

Once the spreading bandwidth is set, the size of □ is controlled by f_m. A compromise between signal reduction desired and tolerable depth of AM yields a range of possible f_m. Another factor in the size of f_m is the resolution bandwidth (RBW) of the spectrum analyzer set by the FCC. The RBW determines the frequency range over which the signal power is calculated. A modulating frequency less than the RBW results

in more than one spectral component within the power calculation range, yielding a power reading higher than that of an f_m greater than the RBW where only one spectral component is present. The modulating frequency must be larger than the RBW, and at the same time small enough to yield the necessary β to arrive at the desired signal reduction.

A. Cancellation of AM Effects

As a case study, an FCC chimney designated between 2.5MHz and 3MHz is studied for the EFL and CHM lamps operating in the MHz range. For proof of concept, a direct digital control platform was developed for the CFL operating at 110kHz. Parameters such as RBW and FCC chimney bandwidth are scaled accordingly.

As predicted, the resulting signal reduction due to FM is not an ideal brick wall response. Figure 12 shows the scaled FCC chimney with two FM signal cases. One has a ΔF=10kHz and a β=20, the other ΔF=5kHz and β=10. Both cases have an fm=500Hz. The case where β=10 better fits the chimney, but distortion caused by AM keeps it from full compliance with the requirement.

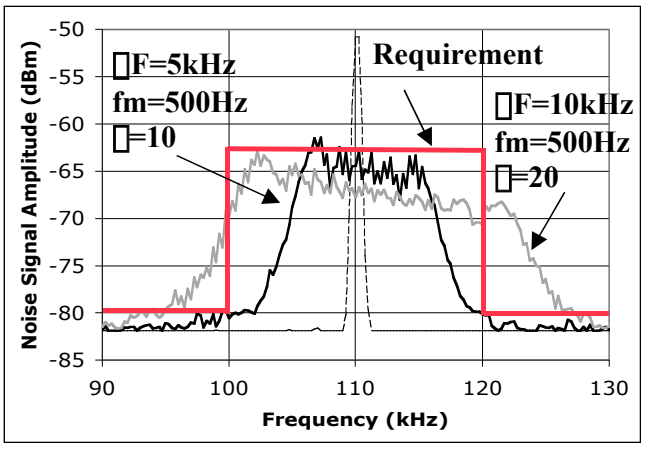

Figure 12. Scaled FCC chimney and two FM cases with β=10 and 20

The solution is to shape the PSD by modifying the modulating waveform. The distortion can by nullified by concentrating more energy in the upper half of the spreading bandwidth. This is accomplished by dwelling longer (providing a shallower slope) in the frequency range above the center or switching frequency.

Figure 13 shows the resulting frequency modulated PSD and ballast current when using a modified modulating waveform. The modified ramp has two different slopes, where 35% of its time is spent in the lower half of the frequency range (105-110kHz) providing a steeper slope, and 65% of its time is spent in the upper half (110-115kHz) providing a shallower slope. The PSD is pre-distorted to compensate for the ballast effects, and results in a 12-15dB reduction of the EMI signal source. In the time domain, shifting the distribution of energy leads to less time spent at the peak current value, reducing component stress.

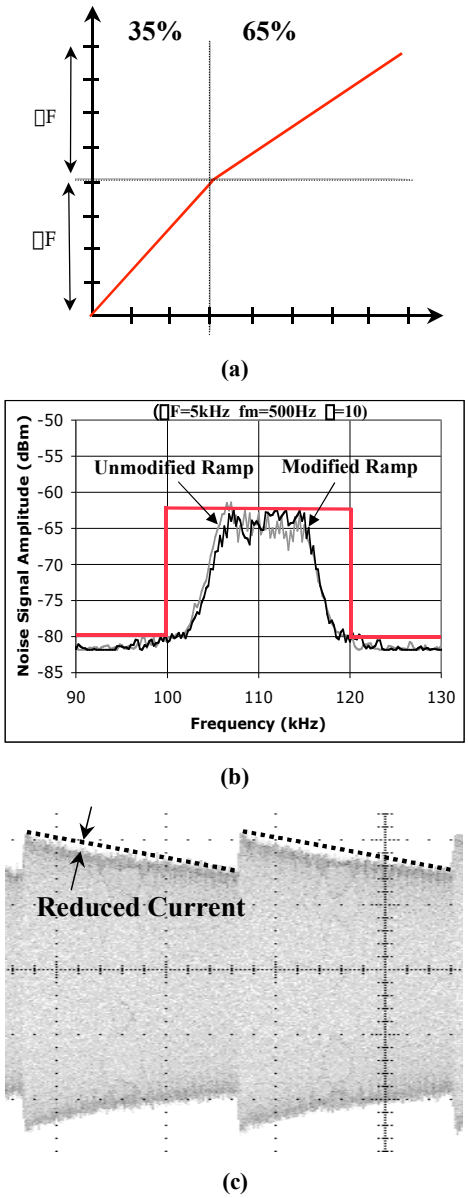

Figure 13. (a) Modified ramp modulating waveform (b) resulting PSD (c) resulting ballast current

II. SUMMARY

Custom spectral shaping of the fundamental in electronic ballasts using FM can aid in the compliance with designated FCC chimneys. Secondary AM effects caused by ballast dynamics can be compensated through modification of the modulating waveform shape, leading to a reduction in both PSD distortion and peak current. Such a modification reduces component stress and adds to the lifetime of the lamp.

As a rule of thumb, the FM modulation index should be between $10 < \beta < 20$ and the modulating waveform frequency should be $f_m >$ RBW to achieve optimal signal reduction. This technique is made practical by direct digital control of the lamp, and is experimentally validated on the CFL system for a specific FCC chimney, where a 12-15dB reduction in signal is achieved.

REFERENCES

[1] Y. F. Yang, L. Yang, C. Q. Yang, "EMI Reduction of Power Supplies by Bi-Frequency Modulation," IEEE Publications 0-7803-1456-5/94, 1994.

[2] T. Tanaka, H. Hamasaki, H Yoshida, "Random-switching Control in DC-to-DC Converters: An Implementation Using Msequence," IEEE Publications 0-7803-3996-7/97, 1997.

[3] K. B. Hardin, J. T. Fessler, D. R. Bush, "Spread Spectrum Clock Generation for the Reduction of Radiated Emissions," IEEE Publications 0-7803-1396-4/94/0000-0041, 1994.

[4] A. C. Wang, S. R. Sanders, "Programmed Pulsewidth Modulated Waveforms for Electromagnetic Interference Mitigation in DC-DC Converters," IEEE Transactions on Power Electronics," Vol. 8, No. 4, October 1993.

[5] K. K. Tse, H. S-H. Chung, S. Y. Hui, H. C. So, "Analysis and Spectral Characteristics of a Spread-Spectrum Technique for Conducted EMI Suppression," IEEE Transactions on Power Electronics, Vol. 15, No. 2, March 2000.

[6] K. K. Tse, H. S. H. Chung, S. Y. Hui, H. C. So, "A Comparative Study of Carrier-Frequency Modulation Techniques for Conducted EMI Suppression in PWM Converters," IEEE Transactions on Industrial Electronics, Vol. 49, No. 3, June 2002.

[7] F. Lin, D. Y. Chen, "Reduction of Power Supply EMI Emission by Switching Frequency Modulation," IEEE Transactions on Power Electronics, Vol. 9, No. 1, January 1994.

[8] T. Ninomiya, M. Shoyama, C. F. Jin, G. Li, "EMI Issues in Switching Power Converters," Proceedings of 2001 International Symposium on Power Semiconductor Devices & ICs, Osaka.

[9] K. K. Tse, H. S. H. Chung, S. Y. Hui, H. C. So, "A Comparative Study of Using Random Switching Schemes for DC/DC Converters," IEEE Publications 0-7803-5160-6/99, 1999.

[10] M. M. Bech, J. K. Pedersen, F. Blaabjerg, A. M. Trzynadlowski, "A Methodology for True Comparison of Analytical and Measured Frequency Domain Spectra in Random PWM Converters," IEEE Transactions on Power Electronics, Vol.14, No. 3, May 1999.

[11] L. Laskaii, P. N. Enjeti, I. J. Pitel, "White-Noise Modulation of High-Frequency High-Intensity Discharge Lamp Ballasts," IEEE Transactions on Industry Applications, Vol. 34, No. 3, May/June 1998.

[12] B. P. Lathi, "Modern Digital and Analog Communication Systems," CBS College Publishing, 1983.

[13] Virtex-II V2MB1000 Development Board User's Guide, Memec, Version 1.3, February, 2002.

[14] R. Erickson, D. Maksimovic, "Fundamentals of Power Electronics," Kluwer Academic Publishers, 2nd ed., 2001

[15] D. Middleton, "An Introduction to Statistical Communications Theory," IEEE Press, New York, 1996